Ain Shams Engineering Journal (2014) 5, 263–270

Ain Shams University

Ain Shams Engineering Journal

www.elsevier.com/locate/asej
www.sciencedirect.com

ENGINEERING PHYSICS AND MATHEMATICS

Electrohydrodynamic capillary instability with heat and mass transfer

Mukesh Kumar Awasthi *

Department of Mathematics, University of Petroleum and Energy Studies, Dehradun, India

Received 24 July 2013; revised 23 August 2013; accepted 1 September 2013
Available online 7 October 2013

KEYWORDS

Capillary instability;
Viscous correction;
Heat and mass transfer;
Axial electric field

Abstract We study the linear analysis of capillary instability of a cylindrical interface between two viscous and dielectric fluids, when the fluids are subjected to a constant axial electric field and, when there is heat and mass transfer across the interface. We use viscous correction for the viscous potential flow theory in which the discontinuities in the irrotational tangential velocity and shear stress are eliminated in the global energy balance by taking viscous contributions to the irrotational pressure. A quadratic dispersion relation that accounts for the growth of axisymmetric waves is obtained and stability criterion is given in terms of a critical value of wave number as well as electric field. It is observed that heat transfer and electric field both have stabilizing effect while vapor fraction has destabilizing effect on the stability of the system.

1. Introduction

A flow is called irrotational flow if fluid particles do not rotate about any axis when they are flowing in a streamline. Hence, the rotational vector for this flow is zero i.e. $\nabla \times \boldsymbol{u} = 0$ and so, velocity $\boldsymbol{u}$ can be expressed as gradient of potential function. Therefore, the viscous term i.e. $\mu\nabla^2\boldsymbol{u}$ in the Navier–Stokes equation is identically zero but the viscosity is not zero, where μ denotes the viscosity the fluid. The irrotational theory that includes the effect of normal viscous stresses at the interface is called viscous potential flow (VPF) theory. To study the capillary instability of a viscous fluid cylinder surrounded by another viscous fluid, Funada and Joseph [1] applied the viscous potential flow theory and observed that the VPF theory gives good agreement with the experimental results. Funada and Joseph [2] also applied the VPF theory to study the capillary instability of viscoelastic fluid of Maxwell type surrounded by a viscous fluid and found that the elastic property of fluid enhances the instability.

The heat and mass transfer phenomenon in multiphase flows has received much attention in recent years because of its wide range of applications in many situations such as boiling heat transfer in chemical engineering and in geophysical problems. Linear stability analysis of the physical system consisting of a vapor layer underlying a liquid layer of an inviscid fluid was carried out by Hsieh [3]. He used the potential flow theory to solve the governing equations but the study was restricted to the inviscid fluids. Nayak and Chakraborty [4] solved the problem of Kelvin–Helmholtz instability but they have taken this problem in the cylindrical geometry.

* Tel.: +91 1332 285157.
E-mail address: mukeshiitr.kumar@gmail.com
Peer review under responsibility of Ain Shams University.

Production and hosting by Elsevier

2090-4479 © 2013 Production and hosting by Elsevier B.V. on behalf of Ain Shams University.
http://dx.doi.org/10.1016/j.asej.2013.09.003

Khodaparast et al. [5] extended the work of Hsieh [3] taking the liquid as viscous fluid while vapor was still inviscid. Awasthi and Agrawal [6] studied the similar problem as taken by Hsieh [3] but they considered both fluids as viscous. The effect of heat and mass transfer on the Kelvin–Helmholtz instability was studied by Asthana and Agrawal [7] when both fluids are miscible and viscous.

Kim et al. [8] extended the work of Funada and Joseph [1] including the effect of interfacial heat and mass transfer. They found that the interfacial heat and mass transfer phenomenon resists the growth of disturbance waves. Awasthi and Agrawal [9] studied the nonlinear effects on the capillary instability when the fluids are miscible and viscous and found the nonlinearity reduces the region of stability.

The viscous stresses in a flow field can be divided into two parts; tangential and normal stresses. If the flow is irrotational, the viscous term in the Navier–Stokes equation is zero but the viscous stresses are not zero. In the VPF theory, we assume that the tangential part of viscous stresses is zero in case of free surface problems but it is not possible in practical situations. To incorporate this discontinuity, Wang et al. [10] included an extra pressure term known as viscous pressure and using the global energy balance, it has been found that this viscous pressure term will include the effect of tangential stresses. This theory is called viscous corrections for the viscous potential flow (VCVPF) theory. Awasthi et al. [11] studied the effect of viscous pressure on the Kelvin–Helmholtz instability of two viscous fluids and found that irrotational tangential stresses have stabilizing effect. It has observed that in case of immiscible and viscous fluids, the stability criterion is same for both VPF and VCVPF theories (Awasthi and Agrawal [12]). If we take the miscible fluids and there is heat and mass transfer across the interface, the effect of viscous pressure will increase the stability of the system (Awasthi [13], Awasthi et al. [14–17]).

The presence of electric field may change the fluid behavior and its flow. The discontinuity of the electric properties of the fluid across the interface affects the force balance at the fluid–fluid interface, which may either stabilize or destabilize the interface depending upon the nature of the fluid and direction of the electric field. The researches show great interest in the field of electrohydrodynamics due to its vast applications in most interesting problems of chemical engineering and other related fields. Electrohydrodynamics also enhances heat transfer which is used in several industrial application including heat exchange manufacturing and power generation. Electrohydrodynamic capillary instability in the presence of heat and mass transfer is widely used for various physical applications such as ink jet printing, paint spraying, pumping fluids, and fuel atomization. The effect of axial electric field on the instability of a liquid jet of finitely conducting and inviscid fluids was examined by Elhefnawy et al. [18]. They have performed the nonlinear analysis and found that if the electric field is uniform, it will stabilize the liquid jet. The combine effect of heat transfer and general electric field on the conducting and inviscid liquid jet instabilities was examined by El-Sayed et al. [19]. They have observed that the effect of radial electric field may stabilize or destabilize the system depending upon the choice of the parameters but axial electric field has stabilizing influence.

To the best of our knowledge, the combined effect of heat transfer and electric field on the capillary instability of two viscous fluids has not been investigated, yet. In the present article, we have made an attempt to study the capillary instability of cylindrical interface of two miscible fluids taking heat and mass transfer into the account and, when the fluids are subjected to uniform electric field acting in the axial direction. In this study, the motion is assumed to be irrotational and fluids are taken as viscous, incompressible and dielectric with different densities, viscosities and permittivities. The effect of gravity and free surface charges at the interface has not been taken into the account. The system has been examined for the axisymmetric disturbances and a quadratic dispersion relation is obtained. Stability criterion has been obtained in terms of critical value of wave number and critical electric field. Various neutral curves have been drawn to show the effect of various physical parameters such as electric field, heat transfer capillary number, on the stability of the system. To study the effect of viscous pressure, the results obtained for the VCVPF analysis have been compared with those obtained for the VPF analysis.

2. Problem formulation

A system of two incompressible, dielectric and viscous fluids, separated by a cylindrical interface, is considered in an annular configuration as shown in Fig. 1. A cylindrical system of coordinates (r, θ, z) is assumed so that in the equilibrium state z-axis is the axis of symmetry of the system. The undisturbed cylindrical interface is taken at radius$R$. In the formulation the superscripts 1 and 2 denote the variables associated with the fluid inside and outside the interface, respectively. In undisturbed state, viscous fluid layer of thickness h_1, density $\rho^{(1)}$, viscosity $\mu^{(1)}$ and permittivity $\varepsilon^{(1)}$ occupies the inner region $r_1 < r < R$ and viscous fluid layer of thickness h_2, density $\rho^{(2)}$, viscosity $\mu^{(2)}$ and permittivity $\varepsilon^{(2)}$ occupies the outer region $R < r < r_2$ where $h_1 = R - r_1$ and $h_2 = r_2 - R$. Surface tension at the interface is taken as σ. The bounding surfaces $r = r_1$ and $r = r_2$ are considered to be rigid. The temperatures at $r = r_1$, $r = R$ and $r = r_2$ are T_1, T_0 and T_2 respectively. Both fluids are assumed to be incompressible and irrotational. In the basic state, thermodynamics equilibrium is assumed and the interface temperature T_0 is set equal to the saturation temperature.

To study the stability of the system, small axisymmetric disturbances are superimposed on the basic rest state. After disturbance, the interface is given by

$$F(r, z, t) = r - R - \eta(z, t) = 0, \tag{1}$$

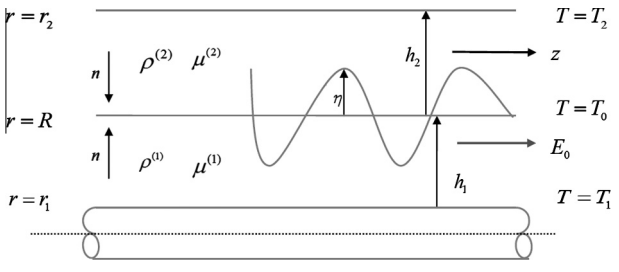

Fig. 1 Equilibrium configuration of the system.

where η, the perturbation in the radius of the interface from the equilibrium value R, and for which the outward unit normal vector is given by

$$\boldsymbol{n} = \frac{\nabla F}{|\nabla F|} = \left\{1 + \left(\frac{\partial \eta}{\partial z}\right)^2\right\}^{-1/2} \left(\boldsymbol{e}_r - \frac{\partial \eta}{\partial z}\boldsymbol{e}_z\right), \tag{2}$$

where $\boldsymbol{e}_r$ and $\boldsymbol{e}_z$ are unit vectors along r and z directions, respectively.

In each fluid layer velocity is expressed as the gradient of the potential function $\phi(r, z, t)$ and the potential functions satisfy the Laplace's equation i.e.

$$\nabla^2 \phi^{(j)} = 0, j = 1, 2, \tag{3}$$

where $\nabla^2 = \frac{\partial^2}{\partial r^2} + \frac{1}{r}\frac{\partial}{\partial r} + \frac{\partial^2}{\partial z^2}$.

The two fluids are subjected to an external electric field E_0, acting along z-axis i.e.

$$\boldsymbol{E} = E_0 \mathbf{e}_z. \tag{4}$$

It is assumed that the quasi-static approximation is valid for the problem, hence the electric field can be derived from electric scalar potential function $\psi(r, z, t)$ such that

$$\boldsymbol{E}_j = E_0 \mathbf{e}_z - \nabla \psi^{(j)}, \quad (j = 1, 2). \tag{5}$$

Gauss's law requires that the electric potentials also satisfy the Laplace's equation i.e.

$$\nabla^2 \psi^{(j)} = 0, \quad (j = 1, 2). \tag{6}$$

The boundary conditions at the rigid cylindrical surfaces $r = r_1$ and $r = r_2$ are given by

$$\frac{\partial \phi^{(j)}}{\partial r} = 0 \text{ at } r = r_j, (j = 1, 2), \tag{7}$$

$$\frac{\partial \psi^{(j)}}{\partial z} = 0 \text{ at } r = r_j, (j = 1, 2). \tag{8}$$

The tangential component of the electric field must be continuous across the interface i.e.

$$[E_t] = 0, \tag{9}$$

where $E_t (= |\mathbf{n} \times \boldsymbol{E}|)$ is the tangential component of the electric field and $[x]$ represents the difference in a quantity across the interface, it is defined as $[x] = x^{(2)} - x^{(1)}$.

There is a discontinuity in the normal current across the interface; charge accumulation within a material element is balanced by conduction from bulk fluid on either side of the surface. The boundary condition, corresponding to normal component of the electric displacement, at the interface is given by

$$[\varepsilon E_n] = 0, \tag{10}$$

where $E_n (= \mathbf{n} \cdot \boldsymbol{E})$ is the normal component of the electric field.

In this analysis, it is assumed that phase-change takes place locally in such a way that the net phase-change rate at the interface is equal to zero. Therefore, the interfacial condition, which expresses the conservation of mass across the interface, is as follows:

$$\left[\rho\left(\frac{\partial F}{\partial t} + \nabla \phi \cdot \nabla F\right)\right] = 0 \text{ at } r = R + \eta, \tag{11}$$

The interfacial condition for energy transfer proposed by Hsieh [3] is expressed as

$$L\rho^{(1)}\left(\frac{\partial F}{\partial t} + \nabla \phi^{(1)} \cdot \nabla F\right) = S(\eta) \text{ at } r = R + \eta, \tag{12}$$

where L is the latent heat released during phase transformation and $S(\eta)$ denotes the net heat flux from the interface. In deriving Eq. (12), it has assumed that the amount of latent heat released depends mainly on the instantaneous position of the interface.

In the equilibrium state, the heat fluxes in positive r-direction in the fluid phases 1 and 2 are $-K_1(T_1 - T_0)/R \ln(R_1/R)$ and $-K_2(T_0 - T_2)/R \ln(R/R_2)$, respectively where K_1 and K_2 denote the heat conductivities of the two fluids. The net heat flux $S(\eta)$ is expressed as (Nayak and Chakraborty [4])

$$S(\eta) = \frac{K_2(T_0 - T_2)}{(R + \eta)(\ln r_2 - \ln(R + \eta))} - \frac{K_1(T_1 - T_0)}{(R + \eta)(\ln(R + \eta) - \ln r_1)}. \tag{13}$$

On expanding $S(\eta)$ about $r = R$ i.e. at $\eta = 0$,

$$S(\eta) = S(0) + \eta S'(0) + \frac{1}{2}\eta^2 S''(0) + \frac{1}{6}\eta^3 S'''(0) + \ldots. \tag{14}$$

Since $S(0) = 0$, from Eq. (13) we get

$$\frac{K_2(T_0 - T_2)}{R\ln(r_2/R)} = \frac{K_1(T_1 - T_0)}{R\ln(R/r_1)} = G, \quad \text{where } G \text{ is a constant.} \tag{15}$$

Hence in the equilibrium state, heat fluxes across the interfaces are equal.

The interfacial condition for conservation of momentum is given by;

$$\rho^{(1)}(\nabla \phi^{(1)} \cdot \nabla F)\left(\frac{\partial F}{\partial t} + \nabla \phi^{(1)} \cdot \nabla F\right) = \rho^{(2)}(\nabla \phi^{(2)} \cdot \nabla F)\left(\frac{\partial F}{\partial t} + \nabla \phi^{(2)} \cdot \nabla F\right) + \left(p_2 - p_1 - 2\mu^{(2)}\boldsymbol{n} \cdot \nabla \otimes \nabla \phi^{(2)} \cdot \boldsymbol{n} + 2\mu^{(1)}\boldsymbol{n} \cdot \nabla \otimes \nabla \phi^{(1)} \cdot \boldsymbol{n} - \frac{1}{2}\left[\varepsilon\left(E_n^2 - E_t^2\right)\right] + \sigma \nabla \cdot \boldsymbol{n}\right)|\nabla F|^2 \quad \text{at} \quad r = R + \eta \tag{16}$$

where p represents the pressure and σ denotes the surface tension. Surface tension has been assumed to be a constant, neglecting its dependence on temperature. Pressure can be obtained using Bernoulli's equation.

3. Viscous correction for the viscous potential flow

To include the effect of irrotational shearing stresses, the viscous pressure has been included in the normal stress balance. The formulation of viscous pressure has been derived from global energy balance.

Let $\boldsymbol{n}_1 = \boldsymbol{e}_r$ be the unit outward normal at the interface for the inner fluid and $\boldsymbol{n}_2 = -\boldsymbol{n}_1$ is the unit outward normal for the outer fluid; and $\boldsymbol{t} = \boldsymbol{e}_z$ be the unit tangent vector. We use the superscripts 'v' for viscous and 'i' for irrotational, respectively. The normal and shear parts of the viscous stress are represented by τ^n and τ^s, respectively.

The mechanical energy equations for outside and inside fluids are respectively

$$\frac{d}{dt}\int_{V_2}\frac{\rho^{(2)}}{2}|\boldsymbol{u}_2|^2dV=\int_A(\boldsymbol{u}_2\cdot\boldsymbol{T}\cdot n_2)dA-\int_{V_2}2\mu^{(2)}\boldsymbol{D}_2:\boldsymbol{D}_2dV$$
$$=-\int_A\left(\boldsymbol{u}_2\cdot\boldsymbol{n}_1(-p_2^i+\tau_2^n)+\boldsymbol{u}_2\cdot\boldsymbol{t}\tau_2^s\right)dV-\int_{V_2}2\mu^{(2)}\boldsymbol{D}_2:\boldsymbol{D}_2dV \tag{17}$$

$$\frac{d}{dt}\int_{V_1}\frac{\rho^{(1)}}{2}|\boldsymbol{u}_1|^2dV=\int_A(\boldsymbol{u}_1\cdot\boldsymbol{T}\cdot\boldsymbol{n}_1)dA-\int_{V_2}2\mu^{(1)}\boldsymbol{D}_1:\boldsymbol{D}_1dV$$
$$=\int_A\left(\boldsymbol{u}_1\cdot\boldsymbol{n}_1(-p_1^i+\tau_1^n)+\boldsymbol{u}_1\cdot\boldsymbol{t}\tau_1^s\right)dV-\int_{V_1}2\mu^{(1)}\boldsymbol{D}_1:\boldsymbol{D}_1dV, \tag{18}$$

where $\boldsymbol{D}_j$ ($j = 1, 2$) is the symmetric part of the rate of strain tensor for inside and outside fluid, respectively.

As the normal velocities at the interface are continuous, $\boldsymbol{u}_2\cdot\boldsymbol{n}_1=\boldsymbol{u}_1\cdot\boldsymbol{n}_1=u_n$, the sum of Eqs. (17) and (18) can be written as

$$\frac{d}{dt}\int_{V_2}\frac{\rho^{(2)}}{2}|\boldsymbol{u}_2|^2dV+\frac{d}{dt}\int_{V_1}\frac{\rho^{(1)}}{2}|\boldsymbol{u}_1|^2dV$$
$$=\int_A\left(u_n(-p_1^i+\tau_1^n+p_2^i-\tau_2^n)+\boldsymbol{u}_2\cdot\boldsymbol{t}\tau_2^s-\boldsymbol{u}_1\cdot\boldsymbol{t}\tau_1^s\right)dA$$
$$-\int_{V_2}2\mu^{(2)}\boldsymbol{D}_2:\boldsymbol{D}_2dV-\int_{V_1}2\mu^{(1)}\boldsymbol{D}_1:\boldsymbol{D}_1dV. \tag{19}$$

On introducing the two viscous pressure correction terms p_1 and p_2 for the inner and outer side of the flow region, we can resolve the discontinuity of the shear stress and tangential velocity at the interface, so

$$\tau_1^s=\tau_2^s=\tau^s \quad \text{and} \quad \boldsymbol{u}_2\cdot\boldsymbol{t}=\boldsymbol{u}_1\cdot\boldsymbol{t}=u_s$$

Hence, Eq. (19) becomes

$$\frac{d}{dt}\int_{V_2}\frac{\rho^{(2)}}{2}|\boldsymbol{u}_2|^2dV+\frac{d}{dt}\int_{V_1}\frac{\rho^{(1)}}{2}|\boldsymbol{u}_1|^2dV$$
$$=\int_A\left(u_n(-p_1^i-p_1+\tau_1^n+p_2^i+p_2-\tau_2^n)\right)dA$$
$$-\int_{V_2}2\mu^{(2)}\boldsymbol{D}_2:\boldsymbol{D}_2dV-\int_{V_1}2\mu^{(1)}\boldsymbol{D}_1:\boldsymbol{D}_1dV. \tag{20}$$

On comparing Eqs. (19) and (20), we get

$$\int_A\left(u_n(-p_1+p_2)\right)dA=\int_A\left(\boldsymbol{u}_1\cdot\boldsymbol{t}\tau_1^s-\boldsymbol{u}_2\cdot\boldsymbol{t}\tau_2^s\right)dA \tag{21}$$

The governing equations of pressure correction are given by :

$$\nabla^2p_j=0 \text{ for } (j=1,2) \tag{22}$$

On solving Eq. (22) using the normal mode method, the expressions for the viscous pressure can be written as:

$$p_1=-(C_kiI_0(kr)+E_kiK_0(kr))\exp(i(kz-\omega t)) \tag{23}$$
$$p_2=-(D_kiI_0(kr)+F_kiK_0(kr))\exp(i(kz-\omega t)) \tag{24}$$

Here $I_0(kr)$ and $K_0(kr)$ denote the modified Bessel functions of the first kind and second kind of order zero, respectively, $i=\sqrt{-1}$ and C_k, E_k, D_k, F_k all denote complex constants.

At the interface $r = R$ the difference in the viscous pressure is given as:

$$-p_1^v+p_2^v=\{(C_k-D_k)iI_0(kR)+(E_k-F_k)iK_0(kR)\}\times\exp(i(kz-\omega t)) \tag{25}$$

We have considered that there exist viscous pressures along with irrotational pressures at the interface of the two fluids. On including the viscous pressure along with irrotational pressure, the equation of conservation of momentum (16) can be written as

$$\rho^{(1)}(\nabla\phi^{(1)}\cdot\nabla F)\left(\frac{\partial F}{\partial t}+\nabla\phi^{(1)}\cdot\nabla F\right)=\rho^{(2)}(\nabla\phi^{(2)}\cdot\nabla F)$$
$$\left(\frac{\partial F}{\partial t}+\nabla\phi^{(2)}\cdot\nabla F\right)+\left(p_2^i+p_2-p_1^i-p_1-2\mu^{(2)}\boldsymbol{n}\cdot\nabla\otimes\right.$$
$$\left.\nabla\phi^{(2)}\cdot\boldsymbol{n}+2\mu^{(1)}\boldsymbol{n}\cdot\nabla\otimes\nabla\phi^{(1)}\cdot\boldsymbol{n}-\frac{1}{2}\left[\varepsilon\left(E_n^2-E_t^2\right)\right]+\sigma\nabla\cdot\boldsymbol{n}\right)$$
$$|\nabla F|^2 \tag{26}$$

Here p_j^i represents irrotational pressure and p_j denotes viscous pressure for inside and outside fluid for ($j = 1, 2$), respectively.

4. Linearization and normal mode analysis

It has been observed that the asymmetric disturbances are always stable for capillary instability. A long cylinder of liquid is unstable to the axisymmetric disturbances with wavelengths greater than $2\pi R$, where R is the radius of the cylinder. Hence, we considered only axisymmetric disturbances in this analysis. Now, axisymmetric disturbances are imposed on the Eqs. (9)–(12) and (26) and retaining the linear terms we can get the following equations.

$$\left[\frac{\partial\psi}{\partial z}\right]=0, \tag{27}$$
$$\left[\varepsilon\left(\frac{\partial\psi}{\partial r}+E_0\frac{\partial\eta}{\partial z}\right)\right]=0, \tag{28}$$
$$\left[\rho\left(\frac{\partial\phi}{\partial r}-\frac{\partial\eta}{\partial t}\right)\right]=0, \tag{29}$$
$$\rho^{(1)}\left(\frac{\partial\phi^{(1)}}{\partial r}-\frac{\partial\eta}{\partial t}\right)=\alpha\eta, \tag{30}$$
$$\left[\rho\left(\frac{\partial\phi}{\partial t}\right)-p+2\mu\frac{\partial^2\phi}{\partial r^2}+\varepsilon E_0\frac{\partial\psi}{\partial z}\right]=-\sigma\left(\frac{\partial^2\eta}{\partial z^2}+\frac{\eta}{R^2}\right) \tag{31}$$

where

$$\alpha=\frac{G}{LR}\frac{\ln(r_2/r_1)}{\ln(r_2/R)\ln(R/r_1)}$$

Now the normal mode technique has been used to find the solution of the governing equations. Letting the interface elevation be represented by:

$$\eta=C\exp(i(kz-\omega t))+c.c., \tag{32}$$

where C represents the amplitude of the surface wave, k denotes the real wave number, ω is the growth rate and $c.c.$ refers the complex conjugate of the preceding term.

On solving Eqs. (3) and (6) with the help of boundary conditions (27)–(30), we get

$$\phi^{(1)} = \frac{1}{k}\left(\frac{\alpha}{\rho^{(1)}} - i\omega\right)E^{(1)}(kr)C\exp(i(kz-\omega t)) + c.c. \quad (33)$$

$$\phi^{(2)} = \frac{1}{k}\left(\frac{\alpha}{\rho^{(2)}} - i\omega\right)E^{(2)}(kr)C\exp(i(kz-\omega t)) + c.c. \quad (34)$$

$$\psi^{(1)} = \frac{i(\varepsilon^{(2)}-\varepsilon^{(1)})E_0\, g_2(k)}{\varepsilon^{(1)}g_2(k)G_1(k) - \varepsilon^{(2)}g_1(k)G_2(k)}(I_0(kr_1)K_0(kr) - I_0(kr_1)K_0(kr))C\exp(i(kz-\omega t)) + c.c. \quad (35)$$

$$\psi^{(2)} = \frac{i(\varepsilon^{(2)}-\varepsilon^{(1)})E_0\, g_1(k)}{\varepsilon^{(1)}g_2(k)G_1(k) - \varepsilon^{(2)}g_1(k)G_2(k)}(I_0(kr)K_0(kr_2) - I_0(kr_2)K_0(kr))C\exp(i(kz-\omega t)) + c.c. \quad (36)$$

where

$$E^{(j)}(kR) = \frac{I_0(kr)K_1(kr_j) + I_1(kr_j)K_0(kr)}{I_1(kR)K_1(kr_j) - I_1(kr_j)K_1(kR)},$$
$$g_j(k) = I_0(kr_j)K_0(kR) - I_0(kR)K_0(kr_j),$$
$$G_j(k) = I_1(kR)K_0(kr_j) - I_0(kr_j)K_1(kR), \quad (j = 1, 2)$$

and symbols I_n and K_n are modified Bessel functions of first and second kind of order $n(=0, 1)$ respectively .

The contribution for the viscous correction is obtained on solving Eq. (21) along with Eq. (25) and we get

$$[(C_k - D_k)iI_0(kR) + (E_k - F_k)iK_0(kR)] = 2kC\left[\mu^{(1)}\left(\frac{\alpha}{\rho^{(1)}} - i\omega\right)E^{(1)}(kR) - \mu^{(2)}\left(\frac{\alpha}{\rho^{(2)}} - i\omega\right)E^{(2)}(kR)\right] \quad (37)$$

5. Dispersion relation

Substituting the values of η, $\phi^{(1)}$, $\phi^{(2)}$, $\psi^{(1)}$, $\psi^{(2)}$ and Eq. (37) in Eq. (31), we get the dispersion relation

$$D(\omega, k) = a_0\omega^2 + ia_1\omega - a_2 = 0 \quad (38)$$

where

$$a_0 = \rho^{(1)}E^{(1)}(kR) - \rho^{(2)}E^{(2)}(kR) \quad a_1 = \alpha(E^{(1)}(kR) - E^{(2)}(kR)) + 2k^2(\mu^{(1)}(F^{(1)}(kR) + E^{(1)}(kR)) - \mu^{(2)}(F^{(2)}(kR) + E^{(2)}(kR)))$$

$$a_2 = \sigma k\left(k^2 - \frac{1}{R^2}\right) + 2k^2\alpha \times \left(\frac{\mu^{(1)}}{\rho^{(1)}}(F^{(1)}(kR) + E^{(1)}(kR)) - \frac{\mu^{(2)}}{\rho^{(2)}}(F^{(2)}(kR) + E^{(2)}(kR))\right) - \frac{k^2E_0^2g_1(k)g_2(k)(\varepsilon^{(2)}-\varepsilon^{(1)})^2}{\varepsilon^{(1)}g_2(k)G_1(k) - \varepsilon^{(2)}g_1(k)G_2(k)}$$

$$F^{(1)}(kR) = E^{(1)}(kR) - \frac{1}{kR}, \quad F^{(2)}(kR) = E^{(2)}(kR) - \frac{1}{kR}$$

After using the transformation $\omega = i\omega_0$, the dispersion relation is obtained in growth rate ω_0 i.e.

$$a_0\omega_0^2 + a_1\omega_0 + a_2 = 0. \quad (39)$$

On application of the Routh–Hurwitz criterion in the Eq. (39) the stability condition is $a_0 > 0$, $a_1 > 0$, $a_2 > 0$.

Using the properties of modified Bessel functions, we have $a_0 > 0$ trivially and since $\mu^{(1)}$ and $\mu^{(2)}$ are positive so $a_1 > 0$.

Hence the condition of stability gives rise to $a_2 > 0$,

$$\left(2k^2\alpha\left(\frac{\mu^{(1)}}{\rho^{(1)}}(F^{(1)}(kR) + E^{(1)}(kR)) - \frac{\mu^{(2)}}{\rho^{(2)}}(F^{(2)}(kR) + E^{(2)}(kR))\right) + \sigma k\left(k^2 - \frac{1}{R^2}\right) - \frac{k^2E_0^2g_1(k)g_2(k)(\varepsilon^{(2)}-\varepsilon^{(1)})^2}{\varepsilon^{(1)}g_2(k)G_1(k) - \varepsilon^{(2)}g_1(k)G_2(k)}\right) > 0 \quad (40)$$

Hence we conclude that the system is stable for $k \geqslant k_c$ and unstable $k < k_c$, where k_c is the critical value of the wave number.

Eq. (40) can also be written as

$$\frac{k_c^2E_0^2g_1(k_c)g_2(k_c)(\varepsilon^{(2)}-\varepsilon^{(1)})^2}{\varepsilon^{(1)}g_2(k_c)G_1(k_c) - \varepsilon^{(2)}g_1(k_c)G_2(k_c)} < \left(2k_c^2\alpha\left(\frac{\mu^{(1)}}{\rho^{(1)}}(F^{(1)}(k_cR) + E^{(1)}(k_cR)) - \frac{\mu^{(2)}}{\rho^{(2)}}(F^{(2)}(k_cR) + E^{(2)}(k_cR))\right) + \sigma k_c\left(k_c^2 - \frac{1}{R^2}\right)\right) \quad (41)$$

It is also concluded that the system is stable for $E \leqslant E_c$ and unstable for $E > E_c$, where E_c is the critical value of the electric field.

The condition for neutral stability is given by

$$2k_c^2\alpha\left(\frac{\mu^{(1)}}{\rho^{(1)}}(F^{(1)}(k_cR) + E^{(1)}(k_cR)) - \frac{\mu^{(2)}}{\rho^{(2)}}(F^{(2)}(k_cR) + E^{(2)}(k_cR))\right) + \sigma k_c\left(k_c^2 - \frac{1}{R^2}\right) - \frac{k_c^2E_0^2g_1(k_c)g_2(k_c)(\varepsilon^{(2)}-\varepsilon^{(1)})^2}{\varepsilon^{(1)}g_2(k_c)G_1(k_c) - \varepsilon^{(2)}g_1(k_c)G_2(k_c)} = 0 \quad (42)$$

For $E_0 = 0$, Eq. (42) is reduced to dispersion relation as obtained by Awasthi et al. [16]. In Eq. (42) putting $E_0 = 0$ and neglecting the effect of shearing stresses, we get the dispersion relation as obtained by Kim et al. [8]. Choosing $\mu_1 = 0$, $\mu_2 = 0$, $\alpha = 0$, $r_1 \to 0$, $r_2 \to \infty$ and $E_0 = 0$, the dispersion relation (42) reduces to form $\omega_0^2 = \frac{T(1-x^2)}{R^3}\left[\frac{xI_1(x)K_1(x)}{\rho^{(1)}I_0(x)K_1(x) + \rho^{(2)}I_1(x)K_0(x)}\right]$, using the results $I_0'(x) = I_1(x), K_0'(x) = -K_1(x), x = kR, \lim_{r_1} \to 0 K_0'(kr_1) \to \infty$, $\lim_{r_2\to\infty} I_0'(kr_2) \to \infty$. Here the condition for stability is $x > 1$, which is well known Rayleigh criteria for a cylindrical jet.

6. Dimensionless form of dispersion relation

Consider the dimensionless variables

$$\hat{r} = r/h, \quad \hat{z} = z/h, \quad \hat{\eta} = \eta/h, \quad \hat{t} = t/\tau, \quad \hat{\omega} = \omega\tau, \quad \hat{k} = kh, \quad \hat{h} = h_1/h = \varphi, \quad \hat{R} = \hat{r}_1 + \varphi,$$

where the length scale h and time scale τ are defined as $h = r_2 - r_1, \tau = \sqrt{\rho^{(2)}h^3/\sigma}$.

Also, if we consider

$$\hat{\rho} = \frac{\rho^{(1)}}{\rho^{(2)}}, \quad \hat{\mu} = \frac{\mu^{(1)}}{\mu^{(2)}}, \quad Oh = \frac{\sqrt{\rho^{(2)}\sigma h}}{\mu^{(2)}}, \quad \hat{\alpha} = \frac{\alpha}{\rho^{(2)}/\tau}, \quad \Lambda = \frac{2\hat{\alpha}}{Oh}, \quad \kappa = \frac{\hat{\mu}}{\hat{\rho}}, \quad \hat{p}_1 = \frac{h^2}{k_1}, \quad \hat{\varepsilon} = \frac{\varepsilon^{(1)}}{\varepsilon^{(2)}}, \quad \widehat{E}^2 = \frac{\varepsilon^{(2)}E_0^2h}{\sigma}$$

where Oh denotes the Ohnesorge number and it is defined as the ratio of the surface tension force to the inertia force, $\hat{\alpha}$ represents the heat transfer capillary number, φ denotes the inner fluid fraction, κ represents the kinematic viscosity ratio and Λ denotes the alternative heat transfer capillary number.

The dimensionless form of Eq. (38) can be written as

$$
\begin{aligned}
&D(\hat{\omega},\hat{k}) = \hat{a}_0\hat{\omega}^2 + i\hat{a}_1\hat{\omega} - \hat{a}_2 = 0\\
&\hat{a}_0 = (\hat{\rho}E^{(1)}(\hat{k}\widehat{R}) - E^{(2)}(\hat{k}\widehat{R}))\\
&\hat{a}_1 = \hat{\alpha}\Big(E^{(1)}(\hat{k}\widehat{R}) - E^{(2)}(\hat{k}\widehat{R})\Big) + \frac{2\hat{k}^2}{oh}(\hat{\mu}(F^{(1)}(\hat{k}\widehat{R}) + E^{(1)}(\hat{k}\widehat{R}))\\
&\quad - (F^{(2)}(\hat{k}\widehat{R}) + E^{(2)}(\hat{k}\widehat{R})))\\
&\hat{a}_2 = \frac{2\hat{k}^2\hat{\alpha}}{oh}\left(\frac{\hat{\mu}}{\hat{\rho}}(F^{(1)}(\hat{k}\widehat{R}) + E^{(1)}(\hat{k}\widehat{R})) - (F^{(2)}(\hat{k}\widehat{R}) + E^{(2)}(\hat{k}\widehat{R}))\right)\\
&\quad + \hat{k}(\hat{k}^2 - \frac{1}{\widehat{R}^2}) - \frac{\hat{k}^2\widehat{E}^2 g_1(\hat{k})g_2(\hat{k})(1-\hat{\varepsilon})^2}{\hat{\varepsilon}g_2(\hat{k})G_1(\hat{k}) - g_1(\hat{k})G_2(\hat{k})}
\end{aligned}
\tag{43}
$$

and non-dimensional form of Eq. (42) is given by:

$$
\left(\Lambda\hat{k}_c\Big(\kappa(F^{(1)}(\hat{k}_c\widehat{R}) + E^{(1)}(\hat{k}_c\widehat{R})) - \Big(F^{(2)}(\hat{k}_c\widehat{R}) + E^{(2)}(\hat{k}_c\widehat{R})\Big)\Big) + \Big(\hat{k}_c^2 - \tfrac{1}{\widehat{R}^2}\Big) - \frac{\hat{k}_c\widehat{E}^2 g_1(\hat{k}_c)g_2(\hat{k}_c)(1-\hat{\varepsilon})^2}{\hat{\varepsilon}g_2(\hat{k}_c)G_1(\hat{k}_c) - g_1(\hat{k}_c)G_2(\hat{k}_c)}\right) = 0 \tag{44}
$$

7. Results and discussion

In this section, the numerical computation has been carried out using the expressions presented in the previous section for a film boiling condition. We have taken vapor and water as working fluids identified with phases 1 and 2, respectively, such that $T_1 > T_0 > T_2$. We are treating steam as incompressible since the Mach number is expected to be small. In film boiling, the vapor-water interface is in saturation condition and the temperature T_0 is equal to the saturation temperature. Following parametric values have been taken:

$\rho^{(1)} = 0.001$ gm/cm^3, $\rho^{(2)} = 1.0$ gm/cm^3,

$\mu^{(1)} = 0.00001$ poise, $\mu^{(2)} = 0.01$ poise, $\sigma = 72.3$ dyne/cm

The diameters of the inner and outer cylinders are taken as 1 cm and 2 cm, respectively. At the interface, phase-change is taking place. Neutral curves for wave number divide the plane into a stable region above the curve and an unstable region below the curve while neutral curves for the magnetic field divide the plane into a stable region below the curve and an unstable region above the curve. In the following the effect of various physical parameters on the onset of instability is interpreted through various Figures.

The effect of alternative heat transfer capillary dimensionless group Λ on the neutral curves for critical wave number has been shown in Fig. 2 when the electric field intensity $\widehat{E} = 5$. Here we have found that if we Λ constant and increase κ, the critical wave number k_c reduces for fixed value of vapor fraction φ; hence the VCVPF theory predicts longer stable waves. As alternative heat transfer capillary dimensionless group Λ increases, the stable region also increases. Since Λ is directly proportional to the heat flux and inversely proportional to the surface tension. Therefore, surface tension has destabilizing effect on the stability of the system while heat flux has stabilizing effect. This is the similar result as one obtained by Awasthi et al. [17] for the capillary instability with heat and mass transfer in the absence of electric field. Therefore, it has been concluded that the behavior of heat transfer across the interface does not affected by the presence of electric field. The effect of heat and mass transfer on the stability of the system can be explained in terms of local evaporation and condensation at the interface. At a perturbed interface, crests are warmer because they are closer to the hotter boundary on the vapor side, thus local evaporation takes place, whereas troughs are cooler and thus condensation takes place. The liquid is protruding to a hotter region and the evaporation will diminish the growth of disturbance waves.

The effect of electric field intensity $\widehat{E}$ on the neutral curves for the critical wave number k_c has been studied in Fig. 3. It has been observed that for a fixed value of κ and Λ, the critical wave number k_c decreases on increasing electric field intensity $\widehat{E}$. Therefore, it is concluded that $\widehat{E}$ has stabilizing effect. If

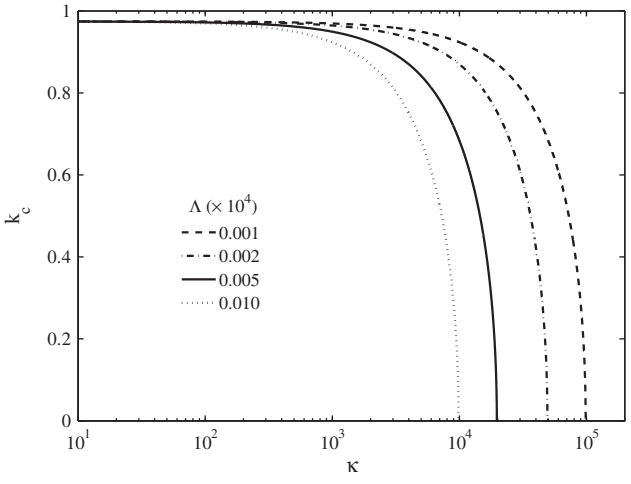

Fig. 2 Neutral curves for critical wave number when $\widehat{E} = 5, \varphi = 0.01$ for the different values of heat transfer capillary number Λ.

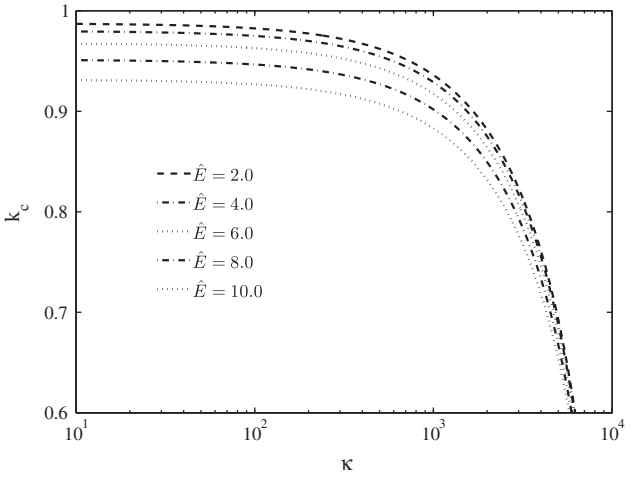

Fig. 3 Neutral curves for critical wave number when $\Lambda = 10^{-6}$, $\varphi = 0.01$ for the different values of electric field intensity $\widehat{E}$.

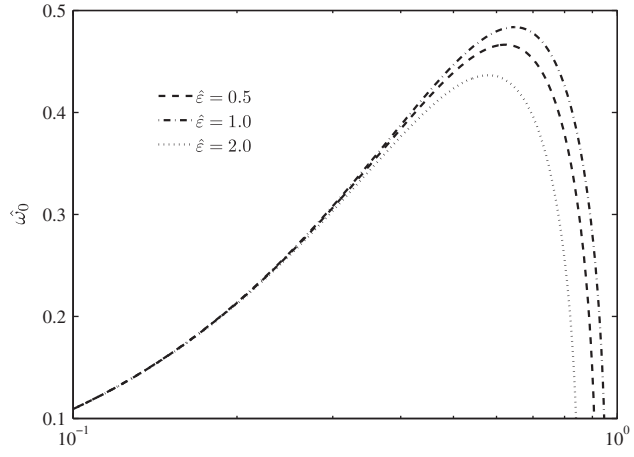

Fig. 4 Growth rate curves when $\hat{\alpha} = 10^{-4}, \widehat{E} = 5, \varphi = 0.01$ for the different values of permittivity ratio of two fluids $\hat{\varepsilon}$.

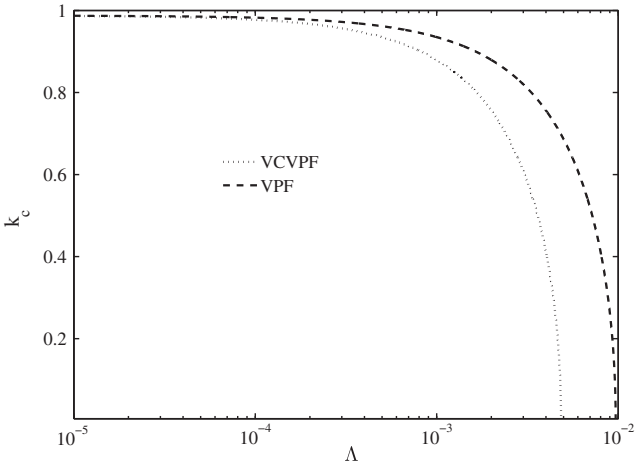

Fig. 6 Comparison between the neutral curves of wave number obtained for VPF and VCVPF solution when $\widehat{E} = 2, \varphi = 0.01$.

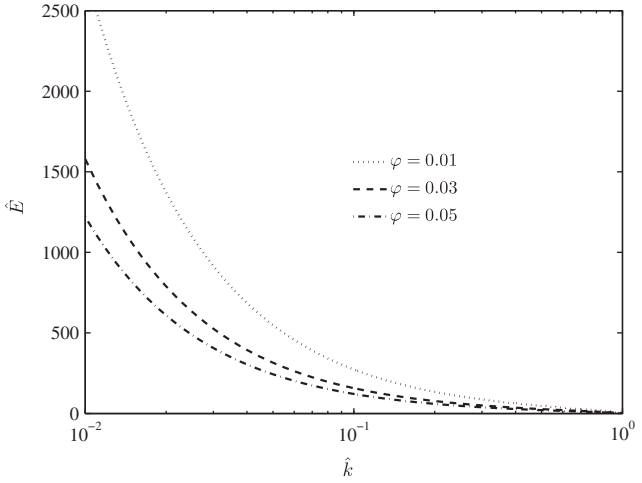

Fig. 5 Neutral curves for critical electric field when $\Lambda = 10^{-6}$ for the different values of vapor fraction φ.

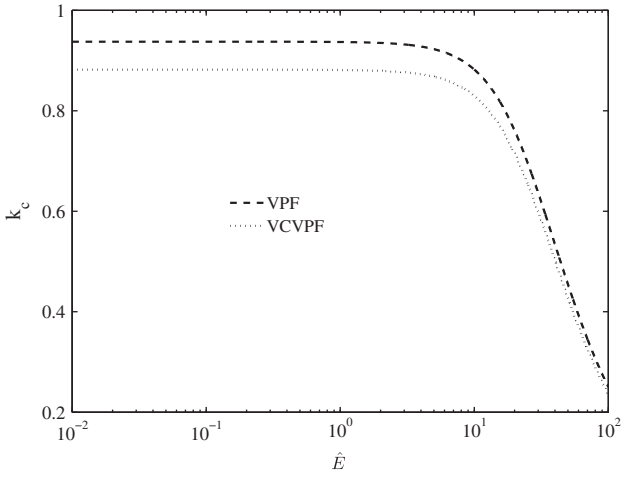

Fig. 7 Comparison between the neutral curves of wave number obtained for VPF and VCVPF solution when $\Lambda = 10^{-6}$, $\varphi = 0.01$.

electric field is present in the analysis, the term contributed from the applied electric field added in the right hand side of the Eq. (42) and so that critical value of wave number decreases and system will become more stable. For a fixed value of vapor thickness φ, on increasing κ, the critical wave number k_c decreases and finally vanishes at threshold κ.

The variation of growth rate $\hat{\omega}_0$ for different values of permittivity ratio of two fluids $\hat{\varepsilon}$ has been shown in Fig. 4 when $\hat{\alpha} = 10^{-4}, \widehat{E} = 2, \varphi = 0.01$. The Figure shows that as the ratio of the permittivities of the two fluids increases, the growth of disturbance wave first increases and after that decreases. It concludes that $\hat{\varepsilon}$ shows dual nature in the stability analysis i.e. destabilizing as well as stabilizing effect. At the constant value of the electric field, the most unstable case was found when both the fluids have same permittivity i.e. $\hat{\varepsilon} = 1$. This happens because at $\hat{\varepsilon} = 1$, the effect of electric field vanishes.

In Fig. 5, we have shown the effect of vapor fraction on the neutral curves of critical value of electric field. As vapor fraction increases, the stable region decreases at the constant value of heat flux and this concludes that the vapor fraction has destabilizing effect on the stability of the system. On increasing the vapor fraction, more heat is supplied to the interface and so the interface becomes unstable. Vapor fraction plays destabilizing role also in the nonlinear analysis of capillary instability when there is heat and mass transfer across the interface as observed by Awasthi and Agrawal [9].

In Fig. 6, the neutral curve of wave number obtained in the VPF analysis has been compared with the neutral curve obtained in the VCVPF analysis when $\widehat{E} = 2, \varphi = 0.01$. It has observed that when heat transfer across the interface is small, both VCVPF and VPF theories predicts same critical wave number k_c but as the heat transfer across the interface increases, the stable region grows for the VCVPF solution as compared to the VPF solution. Therefore, when the heat transfer is very high, the VCVPF solution is more stable than the VPF solution. In the VCVPF solution, the effect of all the viscous stresses (normal as well as shearing stresses) has been taken while in the VPF analysis the effect of shearing stresses

is neglected. Hence, the effect of irrotational shearing stresses will resist the growth of the disturbance waves and system will stabilize.

The comparison between the neutral curve of wave number obtained for the VPF solution and VCVPF solution has been made in Fig. 7 for $\Lambda = 10^{-3}$. It can be seen from the Figure if we kept heat transfer constant, at the lower values of electric field, The VCVPF solution is more stable than the VPF solution but as electric field intensity increases, the VPF and VCVPF solution gives almost same k_c. This is happening because when the electric field intensity is low, the irrotational shearing stresses dominate at the interface while at the higher values of electric field intensity, the polarization force dominates.

8. Conclusion

We have studied the effect of axial electric field on the capillary instability, when there is heat and mass transfer across the interface. The dispersion relation is obtained which is a quadratic equation in growth rate. The stability condition is obtained by applying Routh–Hurwitz criterion. A critical value of electric field as well as critical wave number is obtained. The system is unstable when the electric field is greater than the critical value of electric field, otherwise it is stable. It is observed that the heat and mass transfer has stabilizing effect on the stability of the system and this effect is enhanced in the presence of axial electric field. The heat and mass transfer completely stabilizes the interface against capillary effects even in the presence of electric field. It is also observed that the axial electric field increases the stability of the system. The ratio of dielectric constant has dual effect while vapor fraction destabilizes the system. The heat and mass transfer, for inviscid fluids, has no effect on the stability of the system, while it has stabilizing effect on the stability for viscous fluids. The VCVPF solution is more stable than the VPF solution when electric field intensity is low and heat transfer is high.

References

[1] Funada T, Joseph DD. Viscous potential flow analysis of capillary instability. Int J Multiphase Flow 2002;28:1459–78.

[2] Funada T, Joseph DD. Viscoelastic potential flow analysis of capillary instability. J Non-Newtonian Fluid Mech 2003;111:87–105.

[3] Hsieh DY. Interfacial stability with mass and heat transfer. Phys Fluids 1978;21:745–8.

[4] Nayak AR, Chakraborty BB. Kelvin–Helmholtz stability with mass and heat transfer. Phys Fluids 1984;27:1937–41.

[5] Khodaparast KA, Kawaji M, Antar B. The Rayleigh–Taylor and Kelvin–Helmholtz stability of a viscous liquid–vapor interface with heat and mass transfer. Phys Fluids 1995;7:359–65.

[6] Awasthi MK, Agrawal GS. Viscous potential flow analysis of Rayleigh–Taylor instability with and heat and mass transfer. Int J Appl Math Mech 2011;8:73–84.

[7] Asthana R, Agrawal GS. Viscous potential flow analysis of Kelvin–Helmholtz instability with mass transfer and vaporization. Physica A 2007;382:389–404.

[8] Kim HJ, Kwon SJ, Padrino JC, Funada T. Viscous potential flow analysis of capillary instability with heat and mass transfer. J Phys Math Theor 2008;41:335205, 11pp.

[9] Awasthi MK, Agrawal GS. Nonlinear analysis of capillary instability with heat and mass transfer. Commun Nonlinear Sci Numeric Simulate 2012;17:2463–75.

[10] Wang J, Joseph DD, Funada T. Pressure corrections for potential flow analysis of capillary instability of viscous fluids. J Fluid Mech 2005;522:383–94.

[11] Awasthi MK, Asthana R, Agrawal GS. Pressure corrections for the potential flow analysis of Kelvin–Helmholtz instability. Appl Mech Mater 2012;110–116:4628–35.

[12] Awasthi MK, Agrawal GS. Viscous contribution to the pressure for electro-viscous potential flow analysis of capillary instability. Int J Appl Multi Mech 2011;2:130–45.

[13] Awasthi MK. Viscous corrections for the viscous potential flow analysis of Rayleigh–Taylor instability with and heat and mass transfer. J Heat Transfer – Trans ASME 2013;135:071701 (8 pages).

[14] Awasthi MK, Asthana R, Agrawal GS. Pressure corrections for the potential flow analysis of Kelvin–Helmholtz instability with heat and mass transfer. Int J Heat Mass Trans 2012;55:2345–52.

[15] Awasthi MK, Asthana R, Agrawal GS. Viscous corrections for the viscous potential flow analysis of electrohydrodynamic Kelvin–Helmholtz instability with heat and mass transfer. Int J Appl Electro Mech 2013;42:283–301.

[16] Awasthi MK, Asthana R, Agrawal GS. Viscous corrections for the viscous potential flow analysis of magnetohydrodynamic Kelvin–Helmholtz instability with heat and mass transfer. Euro Phys J A 2012;48:174–83.

[17] Awasthi MK, Asthana R, Agrawal GS. Viscous corrections for the viscous potential flow analysis of capillary instability with and heat and mass transfer. J Eng Math 2013;80:75–89.

[18] Elhefnawy ARF, Agoor BMH, Elcoot AEK. Nonlinear electrohydrodynamic stability of a finitely conducting jet under an axial electric field. Physica A 2001;297:368–88.

[19] El-Sayed MF, Mohamed AA, Metwaly TWN. Effect of general applied electric field on conducting liquid jets instabilities in the presence of heat and mass transfer. Appl Math Comput 2006;172:1078–102.

Mukesh Kumar Awasthi has done his post-graduation in Mathematics from the University of Lucknow in the year 2007. He has obtained his Ph.D degree in Mathematics from Indian Institute of Technology Roorkee in 2012. Currently he is working as an assistant Professor in the Department of Mathematics, University of Petroleum and Energy Studies, Dehradun.